Articles

Study of Magnetic FeAl Nanoparticles Synthesized Using a Chemical Route

Dimple P. Dutta,*,† Garima Sharma,*,‡ A. K. Rajarajan,§ S. M. Yusuf,§ and G. K. Dey‡

Chemistry Division, Materials Science Division, and Solid State Physics Division, Bhabha Atomic Research Centre, Trombay, Mumbai 400 085, India

Received December 2, 2006. Revised Manuscript Received January 15, 2007

In this paper we report the magnetic properties of nanosized intermetallic FeAl particles, prepared by a two-step chemical synthesis route and characterized using X-ray diffraction, conventional and high-resolution transmission electron microscopy (HRTEM), and energy dispersive X-ray spectroscopy (EDX) techniques. The nanoparticles have the same crystal structure (B2) as bulk FeAl. Atomic fringes of the FeAl nanocrystals were observed by using HRTEM. The particles were rectangular in shape with an average length of 20−23 nm. The prepared nanoparticles are found to show magnetization with superparamagnetic behavior arising from the core as well as the surface of these particles. A wide distribution of blocking temperature is evident for these superparamagnetic particles.

Introduction

Iron aluminide (FeAl) intermetallics based on B2 order have been of interest because of their excellent corrosion and oxidation resistance.[1−3] In addition, these alloys exhibit low density and high mechanical strength comparable to most austenitic and ferritic stainless steel.[4−6] Hence, these alloys can be used for various applications requiring good oxidation, carburization, and sulfidation as in automotive exhaust manifolds, hot gas filters, catalytic converters, cutting tools, and so forth. They are much cheaper than stainless steel and have high abrasive wear resistance which find use in agricultural applications.[7] However, structural applications of these intermetallic compounds have been limited because of their low-room-temperature ductility and drop in strength above 600 °C due to embrittlement by moisture in air. In this regard, several studies have been done to combat low ductility at room temperature. These include control of grain size and shape, use of alloying elements such as boron, and the application of oxide or copper coatings.[8] Smaller grain size would lead to superior mechanical properties which would enhance the room-temperature ductility and high-temperature strength of the iron aluminides. Hence the emphasis on synthesis of nanoparticles of these alloys is gaining predominance in recent years.

The structure of FeAl is cubic (CsCl type B2 ordering), in which each iron (Fe) atom has eight aluminum (Al) nearest neighbors and six Fe next nearest neighbors. Ordered bulk FeAl alloys have been reported to be nonmagnetic above 35 atom % Al whereas disordered bulk FeAl alloys exhibit magnetization up to 50 atom % Al.[9] The magnitude of the metallic Fe magnetic ordered moment depends on the number of Fe nearest neighbors, that is, 2.2 μ_B/Fe atom for five or more nearest neighbors and nonmagnetic for Fe atoms with less than four nearest Fe neighbors.[9] It has been reported that the concentration dependence of the average magnetization for an Fe atom with four Fe and four Al nearest neighbors has a magnetic moment of 1.8 μ_B/Fe atom. In the stoichiometric ordered B2 structure, the partial replacement of an Al by an Fe atom creates magnetic moments on the formerly nonmagnetic Fe atoms because the number of the nearest Fe neighbors reaches four Fe atoms.[10]

Iron aluminide nanoparticles which possess superior magnetic properties as compared to nonmagnetic ordered bulk material lead to a novel advanced material that combines unique magnetic properties with high strength and ductility.

* Corresponding authors. E-mail: dimpled@barc.gov.in (D.P.D.); garimas@barc.gov.in (G.S.).
† Chemistry Division.
‡ Materials Science Division.
§ Solid State Physics Division.

(1) McKamey, C. G.; DeVan, J. H.; Tortorelli, P. F.; Sikka, V. K. *J. Mater. Res.* **1999**, *6*, 1779.
(2) Rao, V. S. *Electrochim. Acta* **2004**, *49*, 4553.
(3) Baker, I.; George, E. P. *Proceedings of the International Symposium on Nickel and Iron aluminides: Processing, Properties and Applications*; 1998; p 145.
(4) Stoloff, N. S. *Mater. Sci. Eng. A* **1998**, *258*, 1.
(5) Mckamey, C. G. In *Physical Metallurgy and Processing of Intermetallic Compounds*; Stollof, N. S., Sikka, V. K., Eds.; Chapman and Hall, Thomson Publishing: New York, 1996; p 351.
(6) Deevi, S. C.; Sikka, V. K. *Intermetallics* **1996**, *4*, 357.
(7) Sharma, G.; Limaye, P. K.; Ramanujan, R. V.; Sundararaman, M. *Mater. Sci. Eng. A* **2004**, *386*, 408.
(8) Amils, X.; Nogues, J.; Surinach, S.; Baro, M. D.; Munoz-Morris, M. A.; Morris, D. G. *Intermetallics* **2000**, *8*, 805.
(9) Srinivasan, T. M.; Claus, H.; Viswanathan, R.; Beck, P. A.; Bardos, D. In *Phase Stability in Metals and Alloys*; Rudman, P. S., Stringer, J., Jaffe, R. I., Eds.; McGraw-Hill: New York, 1967; p 151.
(10) Besson, R.; Legris, A.; Morillo, J. *Phys. Rev. B* **2001**, *64*, 174105.
(11) Kirk, K. J. *Contemp. Phys.* **2000**, *41*, 61.

10.1021/cm062858e CCC: $37.00
Published on Web 02/28/2007

Nanomagnets appear to be versatile for a wide range of applications in enlarged data storage, memory elements, sensors, and so forth. Geometry of a nanomagnet has great impact on its magnetic properties resulting from the interplay among different types of magnetic energies. Elongated nanomagnets are of interest for binary data storage applications because they have two stable magnetization states.[11] There are only few reports on the preparation of ordered magnetic FeAl nanoparticles which are spherical in shape.[12−14] El-Shall et al.[12] have prepared spherical FeAl nanoparticles by laser vaporization and condensation of bulk FeAl. The particles are ferromagnetic in nature and show coercivity of the order of 0.005 T at room temperature and around 0.07 T at 5 K. FeAl nanograins, synthesized using the ball milling technique by Kiss et al.,[13] are also magnetic, but the particles did not show any magnetic saturation up to a maximum applied magnetic field of 5 T. Chemical synthesis of spherical FeAl nanoparticles has also been reported,[14] but the particles were found to be nonmagnetic in nature. Solution based methods are preferable since they are cost-effective and can be easily scaled up to industrial proportions compared to the LVCC (laser vaporization controlled condensation) method and less time-consuming as compared to ball milling. In this paper we report the chemical synthesis of rectangular block shaped FeAl nanoparticles that have interesting magnetic property. We also report a detailed characterization of the nanocrystalline phase and its chemical composition. The nanoparticle samples studied here are in solid powder form.

Experimental Section

High purity anhydrous ferric chloride and lithium aluminum hydride were obtained from commercial sources. Reagent grade solvents were used after rigorous drying. The entire reaction was carried out in an argon atmosphere. A solution of anhydrous $FeCl_3$ in a tetrahydrofuran (THF)/toluene mixture (15:85) was heated to 80 °C and added slowly to a suspension of $LiAlH_4$ in THF/toluene (25:75) in a 1:1.7 stoichiometric ratio. A black colloid was formed immediately, and the reaction mixture was warmed to 50 °C for 2 h and then allowed to cool under argon. Stirring was continued for 22 h under argon to ensure homogeneous mixing and complete reduction of the ferric salt. The suspension was filtered under argon atmosphere to remove $AlCl_3$, which is a byproduct of the reaction. The residue was washed thoroughly with hexane and dried in vacuo. It was transferred carefully to a quartz boat in an argon-flushed furnace for heat treatment to remove the other byproduct LiCl, which sublimes at approximately 600 °C. Hence heat treatment was done at 750 °C for 3 h to ensure complete removal of LiCl. The residue was cooled under argon and stored in sealed vials in a desiccator flushed with argon. Extreme precaution was taken to ensure an inert atmosphere during all steps of the reaction to minimize contact with air. The residue obtained from the chemical synthesis route after heat treatment was greyish black in color. The particles were found to be attracted toward the magnet.

X-ray diffraction (XRD) measurements were carried out on a Philips instrument, operating with Cu Kα radiation ($\lambda = 1.5417$ Å) and employing a scan rate of 0.02°/ s in the scattering angular range (2θ) of 20 to ∼70°. The scanning electron microscopy (SEM) examination was done on a Vega-Tescan instrument. Conventional transmission electron microscopy (TEM) was recorded on JEOL 2000FX. High-resolution transmission electron microscopic (HR-TEM) studies were done on JEOL 3000 FX. The FeAl particulates, obtained by chemical synthesis, were dispersed in methanol solution and then deposited on the carbon coated copper grids for TEM studies. The chemical composition of the particles was examined by in situ TEM energy dispersive X-ray (EDX) analysis (Bruker axs).

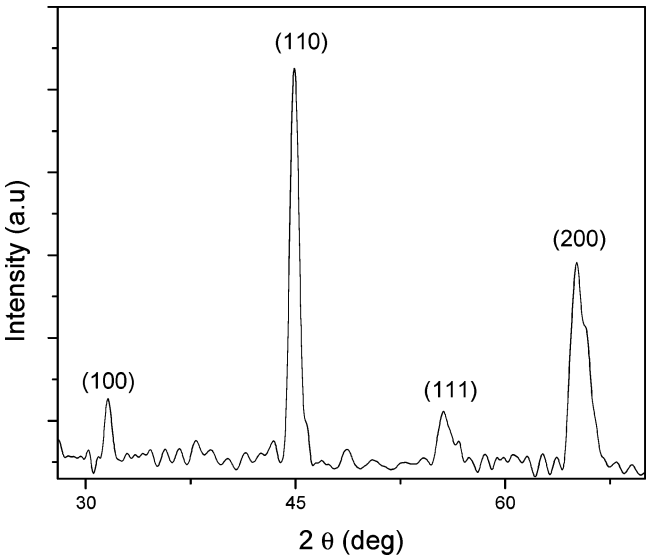

Figure 1. XRD pattern for the FeAl nanoparticles prepared by a chemical synthesis route.

Temperature and magnetic field dependent direct current magnetization measurements were carried out using a vibrating sample magnetometer (VSM), Oxford Instruments, U.K., make. For zero-field-cooled (ZFC) magnetization measurements, the sample was first cooled from room temperature down to 5 K in zero field. After applying the magnetic field of 0.025 T at 5 K, the magnetization was measured in the warming cycle with field on. Whereas for field-cooled (FC) magnetization measurements, the sample was cooled in the same field (0.025 T) down to 5 K, and the FC magnetization was measured in the warming cycle under the same field. Magnetization as a function of field was carried out at room temperature and 5.1 K up to a maximum field of 7 T.

Results and Discussion

Figure 1 shows the XRD pattern of the prepared FeAl nanoparticles. The prominent Bragg peaks at 2θ of 31.17, 44.78, 55.54, and 65.02° correspond to Miller indices (100), (110), (111), and (200), respectively, of B2 ordered FeAl alloy. It is worth mentioning here that no peaks corresponding to metallic Fe were observed in the XRD pattern. The calculated lattice parameter of the FeAl nanoparticles was found to be 2.889 ± 0.001 Å, which showed only a slight deviation from the known lattice parameter for the bulk FeAl (2.895 Å).

The SEM micrograph of the nanoparticles is depicted in Figure 2. It shows that the particles agglomerate into an irregularly shaped submicrometer sized microstructure. Figure 3a shows the conventional TEM image of the FeAl nanoparticles. The individual nanoparticles could not be resolved because of their tendency to agglomerate. Therefore, HRTEM was done to investigate the average size of these

(12) Pithawalla, Y. B.; El-Shall, M. S.; Deevi, S. C.; Strom, V.; Rao, K. V. *J. Phys. Chem. B* **2001**, *105*, 2085.
(13) Kiss, L. F.; Kaptas, D.; Balogh, J.; Bujdoso, L. J.; Gubicza, J.; Kemeny, T. Vincze, I. *Phys. Status Solidi A* **2004**, *201*, 3333.
(14) Pithawalla, Y. B.; Deevi, S. *Mater. Res. Bull.* **2004**, *39*, 2303.

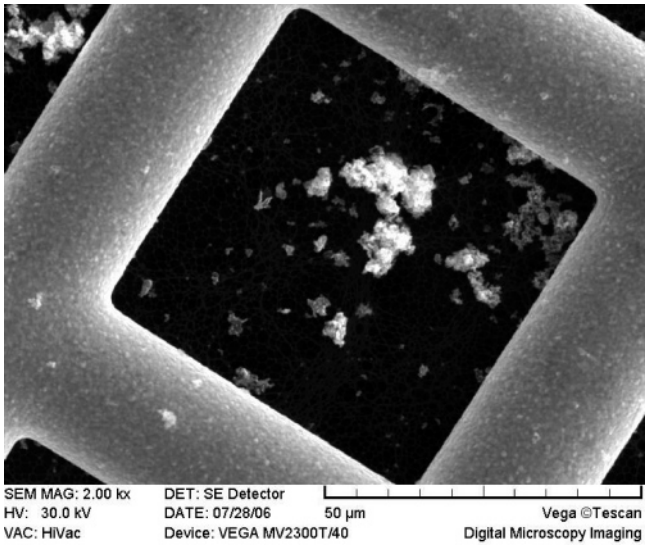

Figure 2. SEM micrograph showing FeAl nanoparticles agglomerate into an irregularly shaped submicrometer sized microstructure.

particles. Figure 3b shows the bright field HRTEM image of the nanoparticle. The corresponding selected area electron diffraction (SAED) pattern confirming the B2 structural atomic ordering in these nanoparticles is shown in Figure 3c. Several HRTEM images were taken into consideration to find the size distribution of the nanoparticles, which were found to be rectangular blocks with an average length in the range of 20-23 nm (Figure 3d). However, the width of the nanoparticles was found to be nearly constant in the range of 3−4 nm. The *d*-spacing for the (100) plane of the FeAl nanoparticles was measured from such images and found to be 2.87 Å, which is in close agreement with the bulk value of 2.90 Å. No oxide layer on the surface of the particles could be seen from the recorded HRTEM images. Our study also confirmed the absence of any amorphous layer on the surface of the nanoparticles. However, the formation of an amorphous layer of Al_2O_3 was reported in the case of particles prepared by LVCC.[12] Figure 4 depicts the in situ TEM EDX pattern of the nanoparticles giving the quantitative information on their chemical composition. The EDX analysis of FeAl nanoparticles collected at six different locations on the sample is shown in Table 1.

Figure 5 shows the temperature dependence of zero field cooled M_{ZFC} and field cooled M_{FC} magnetizations. The peak in the ZFC curve is found at a temperature T_{max} of ∼40 K. A thermo-magnetic irreversibility can be easily seen from the distinct difference between $M_{ZFC}(T)$ and $M_{FC}(T)$ below ∼250 K. This thermo-magnetic irreversibility indicates the onset of the blocking process as found in superparamagnets.[15,16] M_{FC} increases monotonically with lowering of temperature. $M_{FC}(T)$ curves are expected to show rise below the blocking temperature (T_B) for non-interacting superparamagnetic particles, whereas for interacting superparamagnetic particles the FC curve would be flat.[17,18] For superparamagnetic particles at temperatures $T < T_B$, the magnetic moment is blocked along one of the anisotropy directions and does not respond to the applied field, and, hence, the magnetization depends on magnetic history. This causes the difference in FC and ZFC magnetization. In the absence of distribution in the blocking temperature, the branching of M_{FC} and M_{ZFC} is expected to start sharply at T_B. However, a distribution in T_B results in a broad maximum in M_{ZFC} below a branching temperature from where the blocking progresses gradually. At any temperature T, below the branching temperature, the difference of M_{FC} and M_{ZFC} (i.e., ΔM) gives the total magnetization of the nanoparticles that are blocked above T. Hence $d(\Delta M)/dT$ will give the magnetization of the nanoparticles that are blocked in the temperature range of dT around T. The blocking temperature depends on the anisotropy constant and the volume as $T_B = K_aV/25k_B$ where K_a is anisotropy constant, V is the volume, and k_B is the Boltzmann constant.[19] However, with the temperature independent anisotropy factor, the blocking temperature depends only on the volume of individual nanoparticles. A plot of $d(\Delta M)/dT$ represents the particle volume density function. In other words, the plot of ΔM versus T gives the particle volume distribution function and $d(\Delta M)/dT$ gives the particle volume density function. For the nanoparticles with a lower bound for the particle size, a lognormal density function is appropriate to obtain the median blocking temperature and its variance.[16,18,20,21]A fit of the $d(M_{FC} - M_{ZFC})/dT$ versus T data plot, shown in the inset of Figure 5, to a lognormal distribution yields a value of 17 K as the median blocking temperature and 0.6 as the variance.

Figure 6 shows magnetization variation as a function of applied field at room temperature and 5.1 K. The magnetization shows a tendency to saturate above a field of about 0.5 T at room temperature. However, beyond this field (0.5 T) a slight linear increase of magnetization continues until the field measurement limit of 7 T. The slope of the $M(H)$ curve at 5.1 K shows much stronger linear increase over the higher field region (beyond 0.5 T). There is no appreciable hysteresis at room temperature, whereas at 5.1 K a coercivity of about 0.02 T is found (insets of Figure 6). The maximum observed magnetization at 5.1 K under an applied field of 7 T corresponds to 0.32 μ_B/Fe atom as against the expected 2.2 μ_B/Fe atom for pure metallic α-Fe.

Bulk FeAl with the B2 crystal structure does not possesses any magnetization.[9] The observed magnetization behavior for the nanoparticles in the present study can be explained in the following manner. The presence of any strain, lattice distortion, excess vacancies, or impurities can lead to magnetism in ordered FeAl alloys.[22] The presence of point defects in B2 aluminides has also been theoretically proved

(15) Hickey, B. J.; Howson, M. A.; Musa, S. O.; Tomka, G. J.; Rainford, B. D.; Wiser, N. *J. Magn. Magn. Mater.* **1995**, *147*, 253.
(16) Denardin, J. C.; Brandl, A. L.; Knobel, M.; Panissod, P.; Pakhomov, A. B.; Liu, H.; Zhang, X. X. *Phys. Rev. B* **2002**, *65*, 064 422.
(17) Binns, C.; Maher, M. J.; Pankhurst, Q. A.; Kechrakos, D.; Trohidou, K. N. *Phys. Rev. B* **2002**, *66*, 184413.
(18) Mukadam, M. D.; Yusuf, S. M.; Sasikala, R.; Kulshreshtha, S. K. *J. Appl. Phys.* **2006**, *99*, 034310.
(19) Wohlfarth, E. P. *Phys. Lett. A* **1979**, *70*, 489.
(20) Mukadam, M. D.; Yusuf, S. M.; Sharma, P.; Kulshreshtha, S. K.; Dey, G. K. *Phys. Rev. B* **2005**, *72*, 174408.
(21) Mukadam, M. D.; Yusuf, S. M.; Sharma, P.; Kulshreshtha, S. K. *J. Magn. Magn. Mater.* **2004**, *269*, 317.
(22) Reddy, B. V.; Deevi, S. C.; Reuse, F. A.; Khanna, S. N. *Phys. Rev. B* **2001**, *64*, 132408.

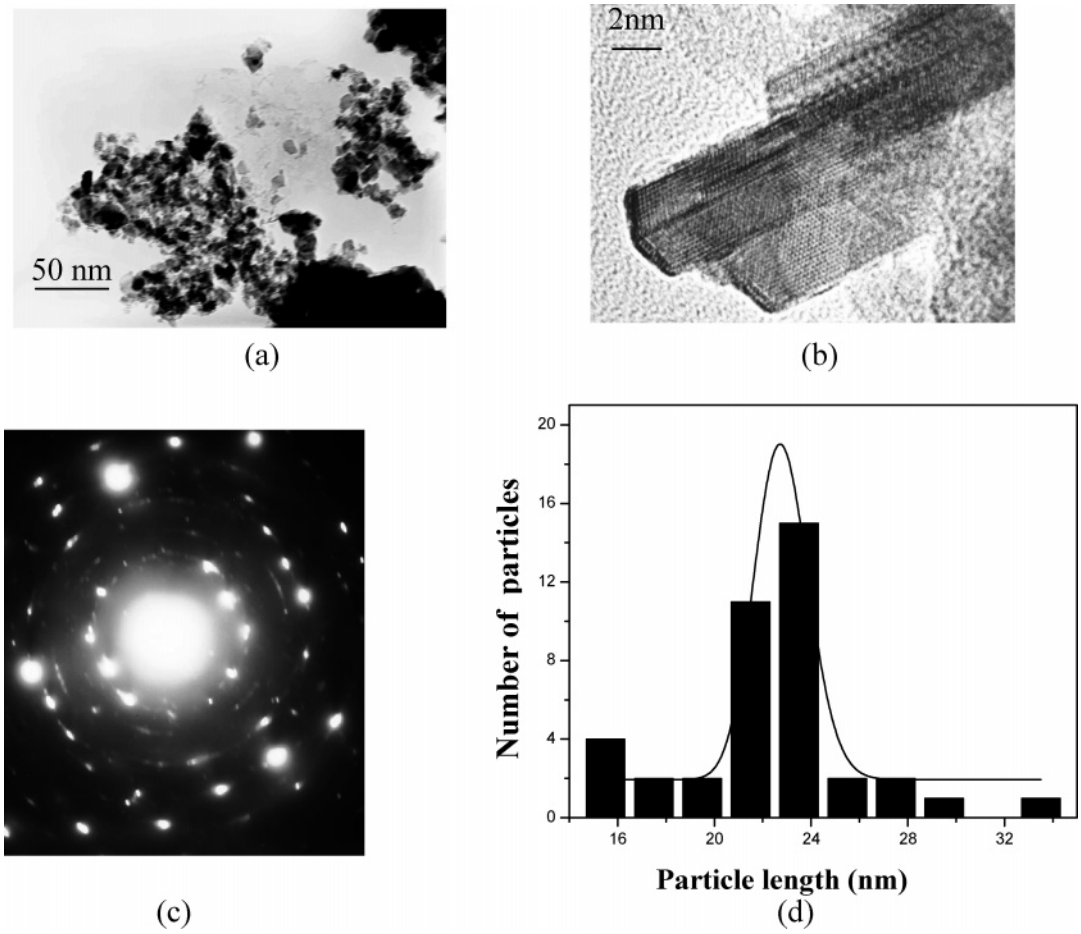

Figure 3. (a) Bright field TEM image of the FeAl nanoparticles, (b) HRTEM image of the individual nanoparticles, (c) the corresponding SAED pattern, and (d) size distribution plot for the FeAl nanoparticles.

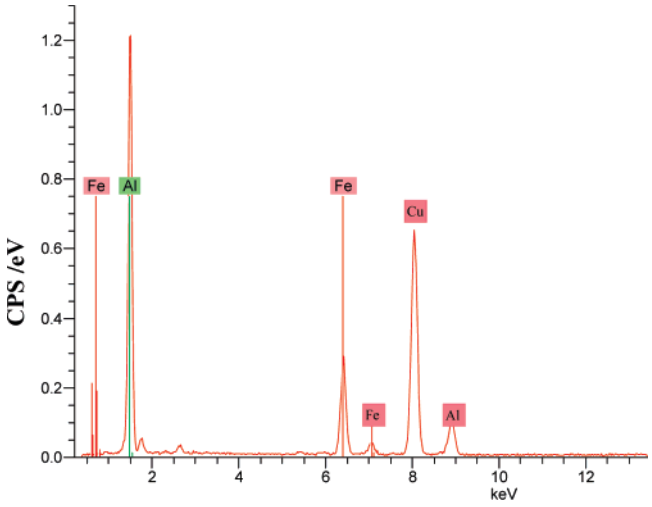

Figure 4. EDX pattern derived from in situ TEM imaging showing the elemental composition of the FeAl nanoparticles. Note: the Cu peak is due to the copper grid on which the samples were dispersed.

Table 1. EDX Data for FeAl Nanoparticles

element	atom %	atom %	atom %	atom %	atom %	atom %
Fe	53.74	54.45	56.89	53.88	54.88	56.12
Al	46.26	45.55	43.11	46.12	45.15	43.88

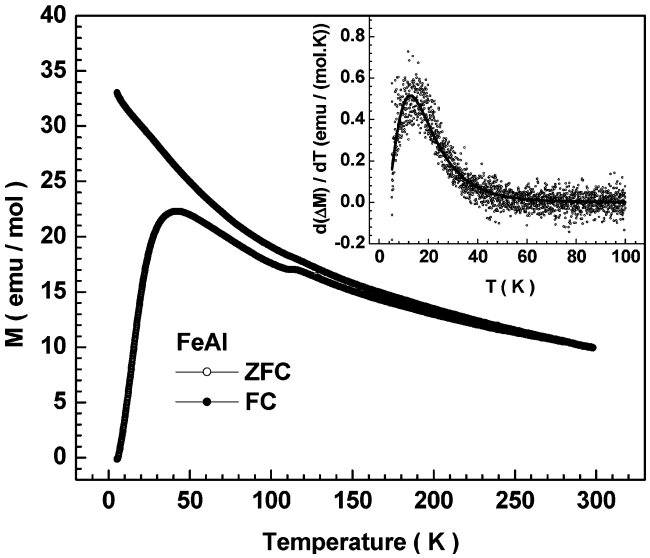

Figure 5. FC and ZFC magnetization curves for FeAl nanoparticles. A lognormal fit to the $d(\Delta M)/dT$ vs $T \equiv d(M_{FC} - M_{ZFC})/dT$ vs T data, derived from the main figure, is shown in the inset.

to enhance the magnetization in these materials.[23] It is known that the preparation of nanoparticles by the ball milling process induces a lot of mechanical strains within the nanograins and hence can induce enhanced magnetization. However, in the present study the nanoparticles were prepared by a chemical synthesis route, and therefore, the particles are expected to be free from any such mechanical distortion and/or strains. Also, the sample in the present study

(23) Kulikov, N. I.; Postnikov, A. V.; Borstel, G.; Braun, J. *Phys. Rev. B* **1999**, *59*, 6824.

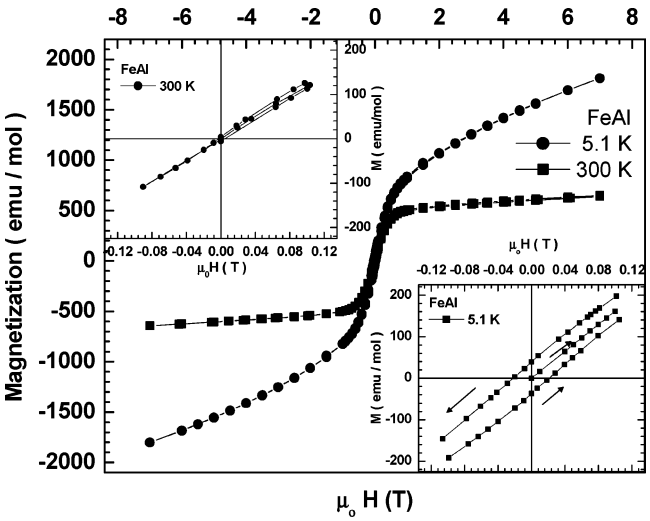

Figure 6. Field variation of magnetization over ±7 T at 300 and 5.1 K for the FeAl nanoparticles. Inset (right) enlarged $M(H)$ curve at 5.1 K showing the presence of hysteresis. Inset (left) enlarged $M(H)$ curve at 300 K showing negligible hysteresis. Joining lines are to guide the eye.

has been found to be free from any contamination (impurities) or disorder as evident from our EDX and XRD measurements. This clearly indicates that the origin of magnetism in our sample is neither strain nor impurities. However, one needs further investigations to find out the reason for the observed magnetism.

The M versus H plot shows interesting features that could be understood on the basis of magnetic contributions from two components of the particles, one coming from the core and the other from the surface. The magnetization from the core part shows a sharp rise at a lower applied magnetic field (∼0.5 T). However, the contribution from the surface is paramagnetic even at low temperature (5.1 K) giving rise to the linear increase of magnetization at high fields. It is found that the slope of the M versus H curve arising from the paramagnetic surface moments is higher at 5.1 K as compared to that at room temperature, which could be explained as a result of the enhancement of the surface moments at lower temperature. The low observed magnetization value at 5.1 K under 7 T applied field can be explained on the basis that the "surface" part could be significant as the dimension of these nanoparticles is of only a few atomic spacings. Further work using microscopic techniques such as neutron scattering is necessary to understand the exact mechanism responsible for the observed magnetization and the effect of particle size and composition on magnetization.

Summary and Conclusion

In this work, we report the synthesis of intermetallic FeAl nanoparticles using a chemical synthesis route. XRD and HRTEM studies confirmed that the nanoparticles have ordered B2 crystalline structure with an average length of 20−23 nm. The magnetic property measurement at 300 and 5.1 K showed that the particles exhibit superparamagnetic behavior with distinct contributions coming from the surface and the core of the particles. A branching between the temperature-dependent ZFC and the FC magnetization curves starts at a significantly higher temperature (∼250 K). The blocking process of these particle moments shows a lognormal distribution of blocking temperature with the median value of 17 K.

Acknowledgment. The authors would like to thank Dr. B.P. Sharma, Associate Director, Materials group, and Dr. S.K. Kulshreshtha, Associate Director, Chemistry Group, for their encouragement to carry out this multidisciplinary work.

CM062858E